Novel Method for Fault Section Identification

E. M. Siavashi, M. R. Baradar, S. Afsharnia, *M. Tavakoli Bina, Senior Member, IEEE

Facualty of Electrical and Computer Engineering , University of Tehran, Tehran, Iran
P. O. Box 14395/515, Tehran 14395–Iran,
*Faculty of Electrical Engineering, K. N. Toosi University of Technology, Tehran, Iran
Email: esiavashi@ut.ac.ir
Email: m.baradar@ece.ut.ac.ir

***Abstract*— From stability point of view fault section identification is an important task for a transmission systems. In this paper, a novel method for section identification using extended Kalman filter (EKF) has been proposed. Subsynchronous frequency as indicator of fault section identification is estimated by EKF algorithm. Several tests as different fault locations have been performed to show performance of the method. Simulation results reveal high performance of the method. In all tests, the proposed algorithm detects accurately presence of subsynchronous frequency.**

***Keywords*—series capacitor, subsynchronous frequency, extended Kalman filter (EKF), fault section identification**

I. INTRODUCTION

Series capacitors (SCs) as one of the solutions have been used widely in power systems. Transient stability of system, power transfer capabilities and the voltage profile improve by series compensation [1]. In spite of many advantages, SCs cause additional problems for protection of series compensated transmission line because of some occurrences such as voltage and current inversion, low-frequency transients and high-frequency transients, etc [2].

Along with series compensation, the metal oxide varistor (MOV), which protects the capacitor from over voltages during faults, acts nonlinearly and increases the complexity of the protection problems. The voltage and current signals produced on the transmission line contain different frequency components. These components include, non-fundamental decaying, as well as decaying DC components due to resonance between the system inductance and series capacitor, subsynchronous frequencies having frequency components varying around half the fundamental frequency value, odd harmonics due to MOV conduction during faults, high-frequency components caused by resonance between line capacitance and line inductance, and fundamental component of the steady-state fault current [3]. Hence, full cycle DFT/Half cycle DFT (FCDFT/HCDFT) or least square error (LSE) methods as conventional techniques fail to process the signals accurately. Therefore, the fundamental phasors are often estimated with large error. Because of dependency on the computation of fundamental voltage and current phasors, effectiveness of the conventional distance protection techniques are limited for series compensated transmission lines.

Above complexities of the protection of series compensated transmission line leads the researchers to propose various techniques in the literature. In [4] is proposed an algorithm based on traveling waves for the protection of series compensated lines. Compensation transmission lines by fixed series capacitor and TCSC based on Neural-network have been suggested in [5] and [6], respectively. In [7] the wavelet transformation (WT) is used to improve protection of series-compensated transmission lines. An algorithm based on high-frequency signals have been proposed in [8] for capturing the high-frequency components of the fault signal. In [9], a voltage compensation-based method has been developed for protection of series compensated transmission lines.

In addition the transient components, steady state components are affected by the series capacitors in the fault loop. Therefore, the apparent impedance calculations should account for the impedances introduced by the MOV-series capacitor combination if they are in the fault loop. On the other hand, if the MOV-series capacitors are not in the fault loop, then the apparent impedance calculations are similar to ordinary transmission lines. As a result, a decision regarding the relative position of the fault with respect to the MOV-series capacitor combination should be taken before the relay starts to calculate the apparent impedance. in that case series capacitor place at the midpoint, the current level may be of the same order at two different fault points of the transmission line (one in front of the capacitor and the other behind it) for the same type of fault. This will result in more complexity while locating the fault point on a transmission system. Therefore, in a series-compensated line, a more reliable fault classification approach is necessary for the fault section; behind or in front of the capacitor [10].

In this paper, a novel method has been proposed for section identification. Since subsynchronous frequency is only induced for faults that include series capacitor, in this method, by detecting subsynchronous frequency from observed current signal, fault section is determined. Extended Kalman filter (EKF) as an observer method is used to detect subsynchronous frequency. This method is fast to detect subsynchronous frequency as well as high accuracy for section identification. For showing effectiveness of this method, MATLAB software is employed.

978-1-4244-4543-1/09/$25.00 ©2009 IEEE

II. ANLYSYS OF SYSTEM MODEL

The fault classification task for the transmission line is divided into two parts; fault-type classification and section identification. An important part of the distance relay is the selector module, responsible for fault identification. Present selectors still suffer from a fairly high rate of misidentification. Thus, for high effectiveness of the relay, it is vital to determine fast and accurately fault section.

When the series capacitors are placed at midpoint of the transmission lines and fault loop, a resonant RLC circuit will be created. Since there is some sort of step change in the system (i.e. fault inception), a natural frequency is going to emerge and compensation is always going to be 100% or less, therefore, the frequency that will be generated is almost always going to be less than 50 Hz. Moreover, this subsynchronous frequency is more than likely not going to be an even sub-multiple of 50 Hz. Hence, it can be difficult to accurately measure the 50 Hz fundamental frequency component of the voltages and currents. When a spectrum is produced using the Fourier Transform, there is a distinct problem caused by frequencies which are close to the fundamental, but not occurring at even sub-intervals detected in a given FFT window.

Fig. 1 illustrates the analytical model that is used in this paper. By neglecting series resistance, the single phase model consists only of a series inductor and capacitor which symbolize the lumped impedance and sum of all series capacitance included in the fault loop.

By considering Fig. 1, when fault occurred at right side of the capacitor, the subsynchronous frequency appears in observed current signal with high frequencies and dc decaying component. Otherwise the signal contains all frequency components except subsynchronous frequency component.

In this section, at first, frequency domain is considered to simplify the analysis of the circuit and finally the response is converted to time domain. Hence, in Fig. 1, inductor and capacitor values replaced by sL_L and $1/sC$, respectively.

Voltage and current be expressed in Laplace domain as follows:

$$V_r = \frac{(V_s)(sL_L + 1/sC)}{(sL_L + sL_S + 1/sC)} \tag{1}$$

$$I_r = \frac{V_s}{(sL_L + sL_S + 1/sC)} \tag{2}$$

Where L_L, L_s and C are a part of transmission line inductance located in fault loop, source inductance and series capacitor, respectively. Also, V_r is voltage and I_r is current that are measured in relay location. By assuming sinusoidal input voltage with unit amplitude, V_s defined in (1) and (2) as below:

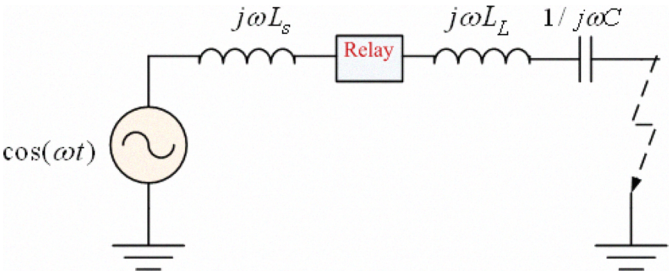

Fig. 1. Equivalent circuit of series compensated transmission line

$$V_s = \frac{s}{s^2 + \omega^2} \tag{3}$$

With substitute (3) in (1) and (2), and taking Laplace conversion, below equations are obtained.

$$V_r(t) = \frac{\cos(\omega t)}{\omega^2 L_S C - 1 + \omega^2 L_L C} + \frac{\cos(\omega t)\omega^2 L_L C}{\omega^2 L_S C - 1 + \omega^2 L_L C} + \frac{L_S \cos\left(\frac{t}{C^{1/2}(L_S + L_L)^{1/2}}\right)}{\omega^2 L_S{}^2 C^2 + 2\omega^2 L_S C^2 L_L - L_S C - L_L C - \omega^2 L_L{}^2 C^2} \tag{4}$$

$$I_r = \frac{C\omega \sin(\omega t)}{\omega^2 L_S C - 1 + \omega^2 L_L C} - \frac{C^{3/2} \sin\left(\frac{t}{C^{1/2}(L_S + L_L)^{1/2}}\right)}{\omega^2 L_S{}^2 C^2 + 2\omega^2 L_S C^2 L_L - L_S C - L_L C - \omega^2 L_L{}^2 C^2} \tag{5}$$

It can be seen that there will be two frequencies present in the voltage, and the same two frequencies present in the current. These radian frequencies are the power system frequency ω, and $1/\sqrt{C(L_s + L_L)}$. This formula of course is a version of the well known $1/\sqrt{CL}$ describing the natural frequency of any resonant series $L - C$ circuit. Second frequency component is determined by percent compensation and a part of line impedance that is located in fault loop. With normal condition and usual levels of series compensation are applied to a transmission line, the alternate frequency generated will be below 50 Hz and thus it is called the subsynchronous frequency.

III. EFFECT OF MOV ON FAULT SIGNAL

Fig. 2 illustrates the series capacitor that is in parallel with MOV and other protection elements. Assume the fixed series capacitor is located close to the midpoint of the transmission line in Fig. 1. The over-voltage protection of series capacitor is provided by the MOV. The characteristics of the MOV may be described by a single exponential model as $i = pv^{\alpha}$. Where α and p are constants.

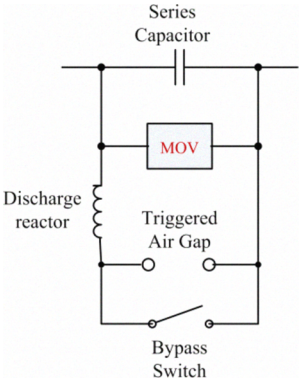

Fig. 2. protective circuit of series capacitor

Due to the presence of the MOV- capacitor at the midpoint of the line, significant differences exist between fault signals on left and right side of the capacitor [11]. Considering a fault on right side of the capacitor (Fig. 1), the transient current signal seen by the relay contains different frequency components. Spectrum analysis of fault signal reveals that odd harmonics is appeared during MOV operation.

As mentioned previously, in this case (right side faults), frequency components consist of : subsynchronous decaying frequency component, odd harmonics caused by MOV conduction during faults, high frequency components caused by resonance between line capacitance and line inductance and Fundamental frequency component. However, for faults on left side of the capacitor (Fig. 1), all aforementioned components except subsynchronous frequency exist in fault current signal. The high frequency components are modeled in all the voltage and current models as white noise with decaying variances [12], [13].

IV. Extended Kalman Filter

Kalman filter estimate the deviations from the nominal trajectory, and hence obtain an estimate of the states of the nonlinear system. This filter is undoubtedly the most widely used nonlinear state estimation technique that has been applied in the past few decades. The extended Kalman filter addresses the problem of estimating the state estimate of a nonlinear system. Consider a nonlinear system with state and measurement equations as (6), (7).

$$x_k = f(x_{k-1}, u_k, w_{k-1}) \tag{6}$$

$$z_k = h(x_k, v_k) \tag{7}$$

In the process equation (6), x is the state of the system, k is the time step, f describes the process model of the system, and w is the process noise. In the measurement equation (7), z is the measurement of the system, h is a nonlinear function that relates the state of the system x to the measurements z, and v is the measurement noise. Notice that the process and measurement noise of the system assumed independent white Gaussian noise with probability distribution matrixes $N(0, Q)$ and $N(0, R)$, respectively. However, the state and the measurement can be approximated as (8), (9).

$$\tilde{x}_k = f(\hat{x}_{k-1}, u_k, 0) \tag{8}$$

$$\tilde{z}_k = h(\tilde{x}_k, v_k) \tag{9}$$

Where $\hat{x}_k$ is the a posteriori estimate of the state from the previous time step $(k-1)$. In a nonlinear system, process function f and measurement function h is linearized about the current state estimate of the system by computing their partial derivatives as follows:

$$x_k \approx \tilde{x}_k + F(x_{k-1} - \hat{x}_{k-1}) + Ww_{k-1} \tag{10}$$

$$z_k \approx \tilde{z}_k + H(x_k - \tilde{x}_k) + V_k v_{k-1} \tag{11}$$

$$F = \frac{\delta f}{\delta x}(\hat{x}_{k-1}, u_k, 0) \tag{12}$$

$$W = \frac{\delta f}{\delta w}(\hat{x}_{k-1}, u_k, 0) \tag{13}$$

$$H = \frac{\delta h}{\delta x}(\tilde{x}_k, 0) \tag{14}$$

$$V = \frac{\delta h}{\delta v}(\tilde{x}_k, 0) \tag{15}$$

Where x and z are the actual state and measurement vectors, $\tilde{x}_k$ and $\tilde{z}_k$ are the approximate state and measurement computed from (8) and (9), F and H are the Jacobian matrices of partial derivatives of f and h with respective to x. Given the linearization of the system, the EKF perform state estimation using a prediction-correction mechanism, as shown in Algorithm 1. At each frame, the filter predicts the current state of the system and correct this estimated state using measurement of the system. The Kalman gain (K_k) is computed to find the optimum feedback gain that minimizes the error covariance between the periori and the posteriori estimation. The updated estimate will then be used to predict the state for the next frame.

V. Signal Model

Since presence of subsynchronous frequency in fault signal is as indicator to identify fault section, equation (2) is used as measure signal to detect subsynchronous frequency. Taking into account previous sections, fault signal contains high frequency components and odd harmonics. In this paper, the high frequency components are modeled in the current model as white noise with decaying variances [12], [13]. Also, for considering the operation of MOV, odd harmonics are inserted in (2).

Algorithm 1: Extended Kalman Filter
Step1: Predict the state with initials: $\hat{x}_k^- = f(\hat{x}_{k-1}, 0)$
Step 2: Compute the error covariance: $P_k^- = F_k P_{k-1} F_k^T + W_k Q_{k-1} W_k^T$
Step 3: Compute the Kalman gain: $K_k = P_k^- H_k^T (H_k P_k^- H_k^T + V_k R_k V_k^T)$
Step 4: Update the state estimate: $\hat{x}_k = \hat{x}_k^- + K_k (z_k - h(\hat{x}_k^-, 0))$
Step 5: Update the error covariance $P = (I - K_k H_k) P_k^-$
Step 6: Return to step 1 with updated measurements

By assuming these conditions, current signal is modeled as below:

$$I_r = \frac{C\omega \sin(\omega t)}{\omega^2 L_S C - 1 + \omega^2 L_L C} - \frac{C^{3/2} \sin\left(\frac{t}{C^{1/2}(L_S + L_L)^{1/2}}\right)}{\omega^2 L_S{}^2 C^2 + 2\omega^2 L_S C^2 L_L - L_S C - L_L C - \omega^2 L_L{}^2 C^2} + \sum_{n=1}^{N} A_{2n+1} \sin((2n+1)\omega t) + \varepsilon \quad (16)$$

Where n and N are natural numbers, A_n is amplitude of nth harmonic and ε represents white noise. Since the amplitude of harmonic components with order more than 5th are low compared to fundamental, in this paper is considered only 3th and 5th harmonic components.

With substituting $\omega_0 = 1/\sqrt{C(L_s + L_L)}$, equation (16) will be changed as below:

$$I_r(t) = \frac{\omega_0^2 \omega C \sin(\omega t)}{\omega^2 - \omega_0^2} - \frac{\omega_0^4 C^{3/2} \sin(\omega_0 t)}{k_1 \omega_0^4 + k_2 \omega_0^2 + \omega^2} + \sum_{n=1}^{N} A_{2n+1} \sin((2n+1)\omega t) + \varepsilon \quad (17)$$

In (17), k_1 and k_2 are constant parameter that are defined as follows:

$$k_1 = -2\omega^2 L_s^3 C^2$$
$$k_2 = 2\omega^2 L_s^2 C - 4\omega^2 L_s C - 2\omega^2 L_s^2 C^2 - 1 \quad (18)$$

Since in this study main objective is tracking of the subsynchronous frequency, for applying EKF in estimation problem, states variables are formed as below:

$$x_1(k) = \omega_0 \quad (19)$$

$$x_2(k) = \frac{\omega_0^2 \omega C \sin(\omega k T_s)}{\omega^2 - \omega_0^2} - \frac{\omega_0^4 C^{3/2} \sin(\omega_0 k T_s)}{k_1 \omega_0^4 + k_2 \omega_0^2 + \omega^2} \quad (20)$$

$$x_3(k) = A_3 \quad (21)$$

$$x_4(k) = A_5 \quad (22)$$

By consideration state variables above, $f(x_k)$ and $h(x_{k+1})$ in (8), (9) are written as follows:

$$f(x_k) = \begin{pmatrix} x_1(k) \\ \frac{x_1^2(k) C \sin(\omega k T_s)}{\omega^2 - x_1^2(k)} - \frac{x_1^4(k) C^{3/2} \sin(x_1(k) k T_s)}{k_1 x_1^4(k) + k_2 x_1^2(k) + \omega^2} \\ x_3(k) \\ x_4(k) \end{pmatrix} \quad (23)$$

$$h(x_k) = x_2(k) + x_3(k) \sin(3\omega k T_s) + x_5(k) \sin(5\omega k T_s) \quad (24)$$

Linearized process and measurement equations are obtained from (12) and (14) as follows:

$$F_k = \begin{pmatrix} 1 & 0 & 0 & 0 \\ M_1 - (M_2 + M_3) & 0 & 0 & 0 \\ 0 & 0 & 1 & 0 \\ 0 & 0 & 0 & 1 \end{pmatrix}$$

$$M_1 = \frac{2x_1(k) C \omega^3 \sin(\omega k T_s)}{(\omega^2 - x_1^2(k))^2}$$

$$M_2 = \frac{t C^{1.5} x_1^4(k) \cos(x_1(k) k T_s) \left[k_1 x_1^4(k) + k_2 x_1^2(k) + \omega^2 \right]}{(k_1 \omega_0^4 + k_2 \omega_0^2 + \omega^2)^2} \quad (25)$$

$$M_3 = \frac{2 C^{1.5} x_1^3(k) \sin(x_1(k) k T_s) \left[k_2 x_1^2(k) + 2\omega^2 \right]}{(k_1 \omega_0^4 + k_2 \omega_0^2 + \omega^2)^2}$$

$$H_k = [0 \;\; 1 \;\; \sin(3\omega k T_s) \;\; \sin(5\omega k T_s)] \quad (26)$$

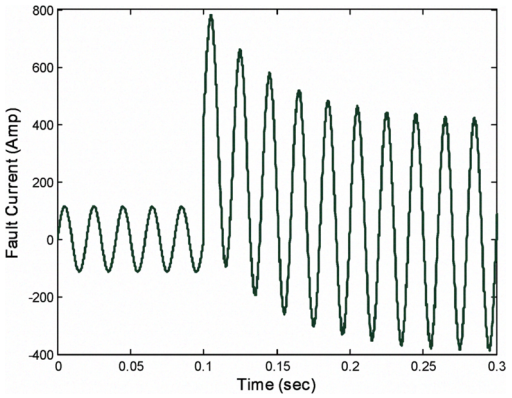

(a)

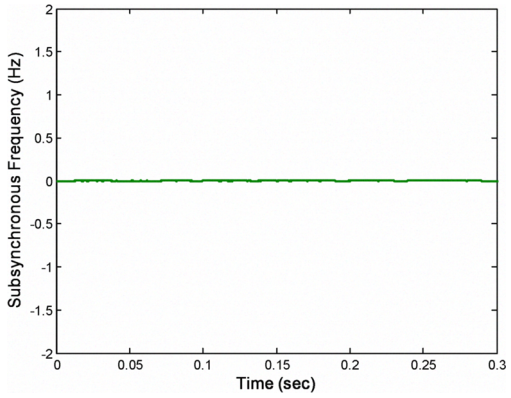

(b)

Fig. 3. Results for test 1 :a) fault current signal

b) estimated subsynchronous frequency

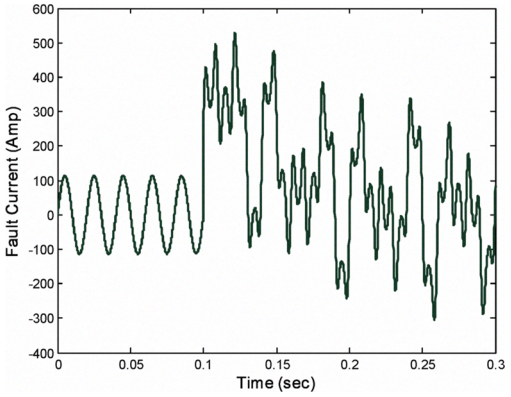

(a)

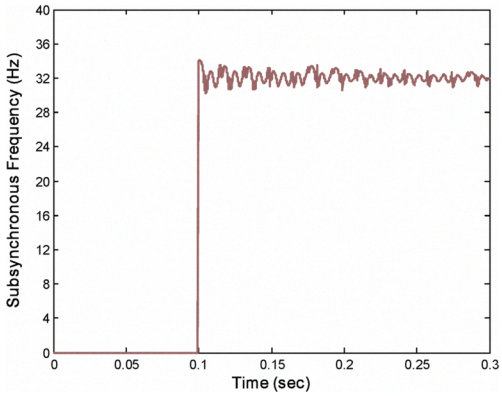

(b)

Fig. 4. Results for test 2 :a) fault current signal

b) estimated subsynchronous frequency

By using (19)-(26), extended Kalman algorithm was applied for tracking subsynchronous frequency as it is shown simulation section.

VI. SIMULATION RESULTS

A 10 kV, 50 Hz voltage source has been considered for all tests. Other value such as Ls, $L_L$and C are 47 mH, 93 mH and 176 uF respectively. Fault time is at 0.1 second; DC decaying component is 350 A with 50 millisecond time constant and for modeling high frequency components, white noise of 60 dB signal-to-noise ratios (SNR) is used. Several tests as different fault locations for validating proposed method are performed.

a) Test 1: A fault on the left side of the capacitor in Fig. 1: As previous sections, when fault occurs on left side of capacitor, subsynchronous frequency is not existent in the fault current.

Fig. 3 shows fault current and estimated subsynchronous frequency. It is seen that estimated frequency for this case is zero as expected. After 0.1 second the nominal peak of current has been increased three times. Also after this time, DC component is added to fault signal.

b) Test 2: A fault on the right side with considering total line inductanceL_L: by considering total L_L, subsynchronous frequency must be 32 Hz. Fig. 4 confirms the performance of proposed method.

However, for fault section identification it is only needed the presence of subsynchronous frequency, not exact value. Therefore, proposed method has high speed response needed for protective relays.

c) Test 3: A fault on the right side with considering two thirds line inductance (L_L): in this case, subsynchronous frequency must be 36 Hz. Fig. 5 reveals the effectiveness of proposed in finding the fault section by detecting subsynchronous frequency.

d) Test 4: A fault on the right side with considering about half line inductance (L_L): fast tracking the frequency by EKF algorithm is shown in Fig. 6. Like as previous tests, in this case, the proposed method has performed fast and accurately, too. It is denoted that all fault current for fault on right side of capacitor consist of sub synchronous frequency, odd harmonics, white noise and DC decaying component.

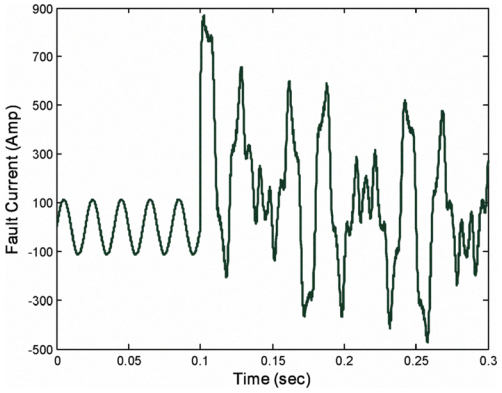

(a)

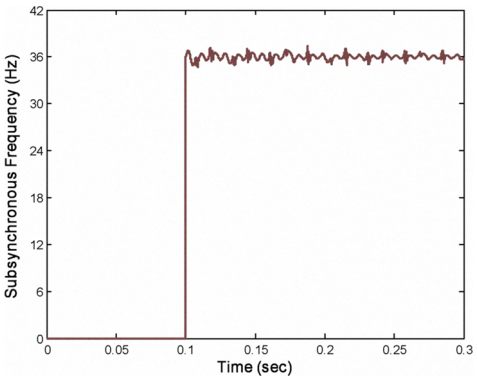

(b)

Fig. 5. Results for test 3:a) fault current signal
b) estimated subsynchronous frequency

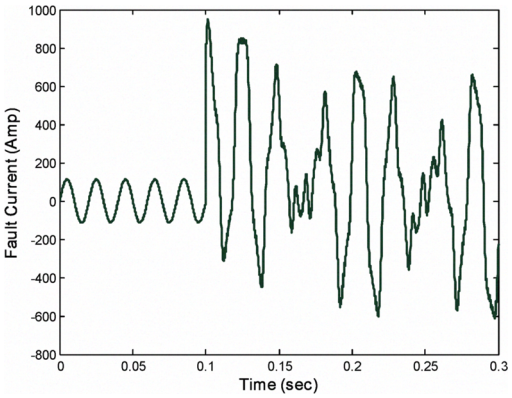

(a)

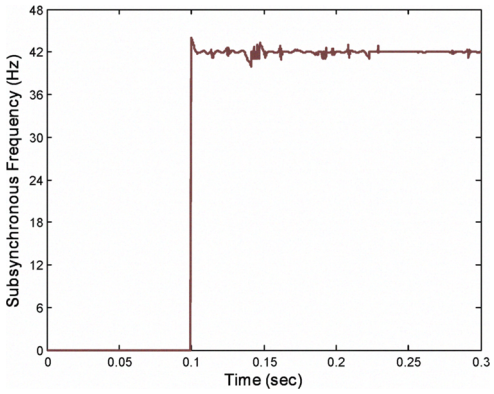

(b)

Fig. 6. Results for test 4 :a) fault current signal
b) estimated subsynchronous frequency

VII. CONCLUSION

In this paper, a novel method for fault section identification using extended Kalman filter has been proposed. Several tests as different fault locations are performed. Effectiveness of this method in detecting subsynchronous frequency as the indicator for section identification by simulation results has been validated.

REFRENCES

[1] W. A. Elmore, Protective Relaying—Theory and Applications, 2nd ed. New York: Marcel-Dekker, 2003.

[2] M. M. Elkateb, W. J. Cheetham, "Problems in the protection of series compensated lines", IEEE Conference Publication on Power System Protection, No. 185, pp.215-220, 1980.

[3] B. Kasztenny, "Distance protection of series compensated lines problems and solutions," in *Proc. 28th Annu. Western Protective Relay Conf.*, Spokane, WA, Oct. 22–25, 2001, pp. 1–36.

[4] D. W. P. Thomas and C. Christopulos, "Ultra-high speed protection of series compensated lines," *IEEE Trans. Power Del.*, vol. 7, no. 1, pp. 139–145, Jan. 1992.

[5] Q. Y. Xaun, Y. H. Song, A. T. Johns, R. Morgan, and D. Williams, "Performance of an adaptive protection scheme for series compensated EHV transmission systems using neural networks," *Elect. Power Syst. Res.*, vol. 36, no. 1, pp. 57–66, Jan. 1996.

[6] Y. H. Song, A. T. Johns, and Q. Y. Xuan, "Artificial neural-network-based protective scheme for controllable series compensated EHV transmission lines," *IEE Proc. Gener. Transm. Distrib.*, vol. 143, no. 6, pp. 535–540, Nov. 1996.

[7] A. I. Megahed, A. M. Moussa, and A. E. Bayoumy, "Usage of wavelet transform in the protection of series-compensated transmission lines," IEEE Trans. Power Del., vol. 21, no. 3, pp. 1213–1221, Jan. 2006.

[8] J. A. S. B. Jayasinghe, R. K. Aggarwal, A. T. Johns, and Z. Q. Bo, "A novel non-unit protection for series compensated EHV transmission lines based on fault generated high frequency voltage signals," *IEEE Trans. Power Del.*, vol. 13, no. 2, pp. 405–413, Jan. 1998.

[9] F. Ghassemi, J. Goodarzi, and A. T. Johns, "Method to improve digital distance relay impedance measurement when used in series compensated lines protected by a metal oxide varistor," *IEE Proc. Gener. Transm. Distrib.*, vol. 145, no. 4, pp. 403–408, Jul. 1998.

[10] A. A. Girgis, A. A. Sallam, and A. K. El-Din, "An adaptive protection scheme for advanced series compensated (ASC) transmission lines," *IEEE Trans. Power Delivery*, vol. 13, pp. 414–420, Jan. 1998.

[11] A Karim El-Din, Digital Protection of Advanced Series Compensated Transmission Lines, Ph D Dissertation, Suez-Canal University, Egypt, 1995.

[12] A. A. Girgis, R. G. Brown, "Modeling of Fault-Induced Noise Signals for Computer Relaying Applications," IEEE Trans on Power Apparatus and Systems, Vol PAS-102, No 9, September 1983, pp2834-2841.

[13] A. A. Girgis and R. G. Brown, "Application of Kalman filtering in computer relaying, " IEEE Trans on Power Apparatus and Systems, Vol PAS-100, pp3387-3397, July,1981.